

# Heat and Mass Transfer in a Falling Film Evaporator with Aqueous Lithium Bromide Solution

M Olbricht\*, J Addy and A Luke

Institute of Technical Thermodynamics, University of Kassel  
Kurt-Wolters-Straße 3, 34125 Kassel, Germany

\*E-mail: m.olbricht@uni-kassel.de

**Abstract:** Horizontal tube bundles are often used as falling film evaporators in absorption chillers, especially for systems working at low pressure as  $\text{H}_2\text{O}/\text{LiBr}$ . Experimental investigations are carried out in a falling film evaporator consisting of a horizontal tube bundle with eighty horizontal tubes installed in an absorption chiller because of a lack of consistent data for heat and mass transfer in the literature. The heat and mass transfer mechanisms and the flow pattern in the falling film are analysed and compared with correlations from literature. The deviations of the experimental data from those of the correlations are within a tolerance of 30%. These deviations may be explained by a change of the flow pattern at a lower Reynolds number than compared to the literature.

## 1. Introduction

Absorption chillers become more and more attractive as an alternative to vapour compression cycles for industrial cold production due to increasing energy costs and rigorous regulations about the emission of greenhouse gases. These cycles are driven by heat instead of electrical energy so that waste heat can be utilised for cooling applications. Waste heat at low temperatures between 60°C and 120°C is a result of many production processes. The appropriate working fluid pair for the absorption process is water/ lithium bromide corresponding to this temperature level.

One of the main challenges in the application of absorption chillers are still their high production costs based on the complex cycle design. These costs are reduced by an improved design of the single components of the absorption chiller. The precise dimensioning of all heat exchangers may have a considerable impact on the economic success of this technology. Most investigations of the heat transfer characteristics of the heat exchangers in the cycle under typical working conditions focus on the absorber. An insufficient design of the evaporator or generator would lead to a bottleneck in the cycle although the absorber is often recognized as the critical component in the process. Due to low pressure in the process and the high surface tension of the working fluid, convective boiling is the main heat transfer mechanism in the evaporator which is less effective in comparison to nucleate boiling.

Adapted to the heat transport process, internally heated, horizontal tube bundles are commonly used as falling film evaporators with the working pair  $\text{H}_2\text{O}/\text{LiBr}$ . Unfortunately, only few data of the heat transfer mechanisms under typical conditions in an absorption cycle are found in the literature. However, models for the heat transfer characteristics of other working fluids under different conditions for horizontal falling film evaporators are reported in the literature [1] [2] [3]. In the following work, experimental investigations are carried out in a falling film evaporator used as



generator in an absorption cycle to evaluate the applicability of these models on the conditions in the cycle. Additionally, the flow pattern of the falling film is examined to validate the influence of the strong polar character of the working fluid and the associated high surface tension on the falling film.

## 2. Experimental Apparatus and Procedure

The experimental investigations are carried out on a newly-developed absorption chiller. A short description of the cycle with a focus on the generator is presented. More detailed information about the whole test rig is given by Olbricht and Luke [4] [5].

The absorption chiller is designed as single effect unit. It consists of an evaporator, absorber, generator and a condenser, which are designed as tube bundle heat exchangers. A schematic view of the cycle is shown in figure 1(left). The generator is basically a falling film evaporator working with aqueous lithium bromide solution as shown in figure 1. All experimental investigations discussed hereafter are related to this apparatus. The vapour, produced by the generator, is pure water due to the negligible small vapour pressure of the lithium bromide. An additional plate heat exchanger is used as solution heat exchanger is included in the cycle to increase its efficiency.

The generator tube bundle heat exchanger consists of 80 parallel tubes and is manufactured of drawn copper tubes with an outer diameter of 12mm. The spacing between the tubes in horizontal and vertical direction is 12mm. The tubes are arranged in 8 parallel tube columns. Each column is designed as a vertical row of 10 horizontal tubes and is built as a tube meander as shown in figure 1(right). The tubes are internally heated by water. The solution film on the outside of the tubes is dispensed by a solution distribution unit.

The temperature of the cold water, coolant and hot water and the flow rate of the solution in the generator, as shown in figure 1, are the varying parameters during the test operation. For the investigation of the heat and mass transfer characteristics, the pressure in the generator, the temperatures and concentrations at the inlet and outlet of the generator and the flow rate of the solution are measured. The concentration of the solution at the inlet and outlet of the generator is determined from samples of the solution which are analysed in an external density meter under defined conditions. The concentration is calculated from the density by the equation of state from Patek and Klomfar [6]. The heat source of the whole cycle is a hot water supply. The inlet and outlet temperature and the volume flow of the hot water which supplies the generator with heat are measured to calculate an overall energy balance of the generator. Photos of the solution flow on the tube bundle are taken through a sight glass for a visual investigation of the flow pattern.

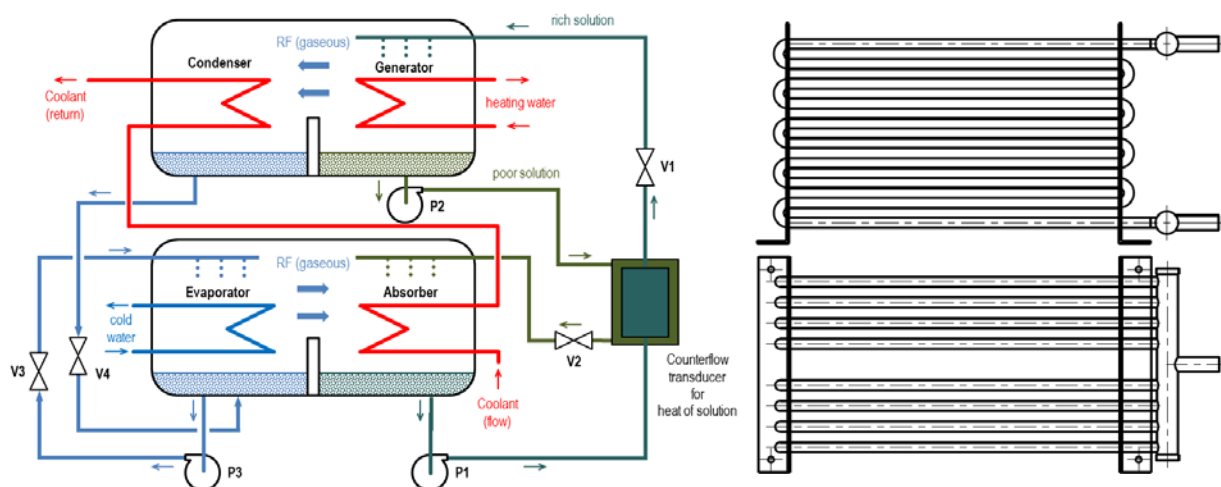


**Figure 1.** Schematic view of the absorption cycle (left), design of the generator heat exchanger (right)

### 3. Data Reduction

The heat transfer coefficient in the falling film

$$\alpha_f = \left[ \frac{1}{k} - \frac{d_o}{d_i \cdot \alpha_h} - \frac{d_o}{2 \cdot \lambda_{cu}} \cdot \ln \frac{d_o}{d_i} \right]^{-1} \quad (1)$$

is calculated from the overall heat transfer coefficient to quantify the heat transfer characteristic of the generator. The overall heat transfer coefficient of the generator

$$k = \frac{\dot{Q}}{A_o \cdot \Delta T} \quad (2)$$

is defined as the heat flux transferred through the outer surface of the tube bundle  $A_o$  by the driving temperature difference  $\Delta T$ . The heat flux

$$\dot{Q} = \dot{m}_h \cdot c_{p,h} \cdot (T_{h,o} - T_{h,i}). \quad (3)$$

is determined from the energy balance of the heating water. The logarithmic mean temperature difference

$$\Delta T_{lm} = \frac{(T_{h,o} - T_{s,i}^{eq}) - (T_{h,i} - T_{s,o}^{eq})}{\ln \left( \frac{(T_{h,o} - T_{s,i}^{eq})}{(T_{h,i} - T_{s,o}^{eq})} \right)} \quad (4)$$

is used as driving temperature difference. Despite the common definition, the equilibrium temperature of the solution at the inlet and outlet is used instead of the measured temperature. This temperature is calculated from the concentrations of the solution at the inlet and outlet and from the pressure in the generator. As shown in eq. (1), the heat transfer coefficient of the hot water  $\alpha_h$  which flows internally through the tube bundle, has to be known and can be predicted by the equation of Gnielinski [7]

$$Nu_i = \frac{\alpha_i \cdot d_i}{\lambda_h} = \frac{(\xi/8) \cdot (Re_i - 1000) \cdot Pr}{1 + 12,7 \cdot \left( \frac{\xi}{8} \right)^{0,5} \cdot (Pr^{\frac{2}{3}} - 1)} \quad (5)$$

for single phase heat transfer in turbulent flow inside round tubes, with the friction factor  $\xi$  calculated by the approach of Colebrook [8] as

$$\xi = (0,782 \cdot \ln(Re_i - 1,51))^{-2}. \quad (6)$$

The test conditions during the experimental investigations fit in all cases to the restrictions of both equations concerning the Re-number and Pr-number. The Re-number is defined as

$$Re_i = \frac{4 \cdot \dot{m}_h}{j \cdot \pi \cdot d_i \cdot \eta_h} \quad (7)$$

where  $j$  represents the number of parallel tube columns in the generator heat exchanger. The total heating water mass flow  $\dot{m}_h$  is equally distributed to the single tube columns. The Pr-number is defined as

$$Pr = \frac{\eta_h \cdot c_{p,h}}{\lambda_h} \quad (8)$$

The film Re-number of the falling film is defined as the fraction of the solution and the mass flow per unit length tube on each side and the dynamic viscosity of solution. The solution mass flow  $\dot{m}_s$  in eq. (10) represents the mass flow per tube column.

$$Re_f = \frac{4\dot{\Gamma}_s}{\eta_s} \quad (9) \quad \text{with} \quad \dot{\Gamma} = \frac{\dot{m}_s}{2 \cdot l} \quad (10)$$

The Nu-number which characterize the heat transfer in the solution film is defined in analogy to falling film heat transfer on vertical tube as

$$Nu_f = \frac{\alpha_f}{\lambda_s} \cdot \left( \frac{\eta_s^2}{g \cdot \rho_s^2} \right)^{1/3} \quad (11)$$

A definition of all variables is given in the nomenclature.

## 4. Results

Based on the design of the test rig the system parameters of the whole absorption chiller can be controlled during the experimental work but not the conditions of the solution at the inlet of the generator in particular. However, a detailed comparison between predicted heat transfer coefficients and measured ones under typical working conditions of the absorption chiller is presented.

### 4.1. Heat Transfer

The parameters of the experimental investigations are the mass flow of the solution per unit length, the Re-number and the heating water inlet temperature.

The heat transfer coefficient of the generator is shown as a function of the mass of the solution flow per unit length for different heating water temperatures in figure 2. The process conditions for this case are: The cold water temperature at the inlet of the evaporator of the absorptions chiller is 15°C and the coolant temperature at the inlet of the absorber is 27°C. The pressure  $p$  in the generator varies between 44-55mbar and the concentration  $x$  of the solution between 0,52-0,60 kg<sub>LiBr</sub>/ kg<sub>solution</sub> depending on the operation point. The heat transfer coefficient increases with higher mass flow rates. This effect results of the improvement of the wetting of the heat exchanger surface with increasing solution mass flow. The heat is only transferred by evaporation from the liquid film on the wetted area of the heat exchanger. Furthermore, the convective heat transfer in the film is enhanced by local turbulences by the droplets and waviness with increasing mass flow of the solution and growing film thickness as shown in figure 3. The slightly degressive trend of the heat transfer coefficient in figure 2 for a high mass flow is a result of a completely wetted heat exchanger surface. Since the thickness of

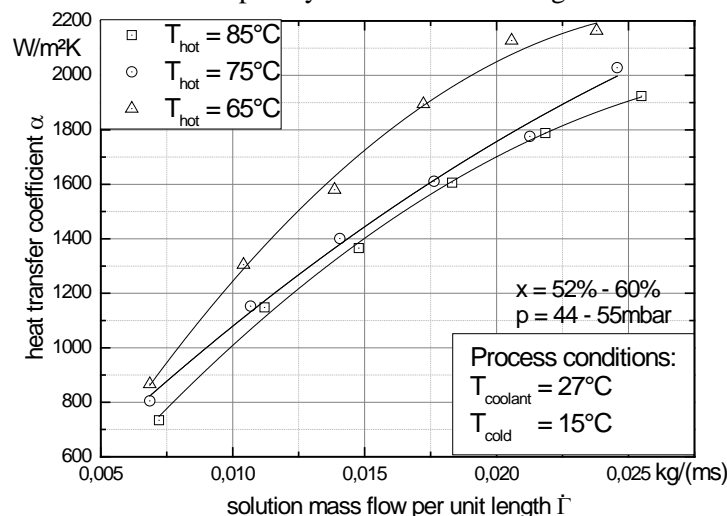


**Figure 2.** heat transfer coefficient as a function of the solution mass flow per unit length tube for different heating water temperatures

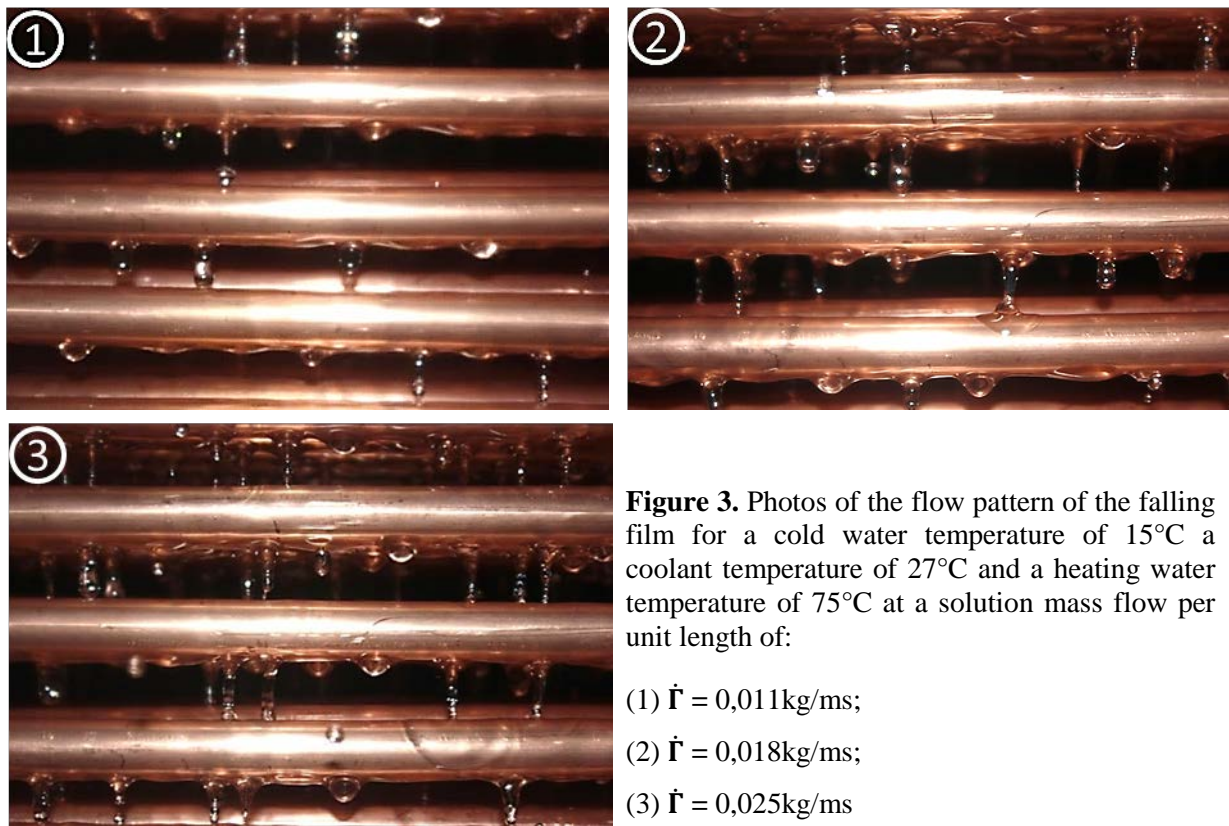


**Figure 3.** Photos of the flow pattern of the falling film for a cold water temperature of 15°C a coolant temperature of 27°C and a heating water temperature of 75°C at a solution mass flow per unit length of:

(1)  $\dot{\Gamma} = 0,011\text{kg/ms}$ ;

(2)  $\dot{\Gamma} = 0,018\text{kg/ms}$ ;

(3)  $\dot{\Gamma} = 0,025\text{kg/ms}$

the film is the main resistance, a further enhancement of the heat transfer coefficient is not possible due to better wetting, but only by more turbulence in the film. An additional reason is the change of the flow pattern in the film. As shown in figure 3 jets appear beside the droplets in the falling film at a solution mass flow per unit length of 0,025 kg/ms. These jets are still instable and often exist just for a few seconds. Jets are developed if the droplets coalesce with the liquid film below during their growth due to high adhesive forces. This process is observed for larger droplets of a certain size and leads to a decrease in the quantity of single droplets. The turbulence and waviness of the film increases with higher thickness of the film although the number of droplets decreases. This leads to a depressive increase of the heat transfer coefficient for a high solution mass flow.

The interaction between the generator and the whole absorption cycle is discussed by the investigation of the dependence of the heat transfer coefficient on the hot water temperature. An improvement of the heat transfer coefficient with decreasing heating water temperature is shown in figure 2. With decreasing hot water temperature, the inlet temperature of the solution and the concentration of LiBr in the solution decrease. This leads to a lower viscosity and thereby to an increase of the Re-number according to eq. (7). Higher Re-numbers indicate more turbulence in the falling film and an enhancement of the heat transfer.

#### 4.2. Comparison with literature

The experimental data are compared with correlations for the heat transfer in horizontal tube bundle falling film evaporators to evaluate their applicability for evaporation of aqueous LiBr-solution at low pressure conditions in an absorption chiller. Selected correlations, which are developed from experimental data of the working fluid water or with fluids having similar material properties, are taken from literature [1], [2] and [3] and are listed in table 1. Data of these working fluids are chosen to consider the polar character of the fluid and the high surface tension.

**Table 1.** Correlations for heat transfer in falling films on horizontal tubes

Author	Correlation	Eq.
Sernas [1]	$Nu = 0,01925 \cdot Re^{0,24} \cdot Pr^{0,66}$	(12)
Hu and Jacobi (Droplet) [2]	$Nu = 0,113 \cdot Re^{0,85} \cdot Pr^{0,85} \cdot Ar^{-0,27} \cdot \left(\frac{s}{d}\right)^{0,04}$	(13)
Hu and Jacobi (Jet) [2]	$Nu = 1,378 \cdot Re^{0,42} \cdot Pr^{0,26} \cdot Ar^{-0,23} \cdot \left(\frac{s}{d}\right)^{0,08}$	(14)
Jani [3]	$Nu = 0,7893 \cdot Re^{0,16587} \cdot Pr^{0,37275} \cdot Sc^{-0,041769} \cdot D^{*-0,4335}$	(15)

The turbulence degree as well as the relation between velocity and temperature boundary layer are taken into account in all correlations by the Re-number and the Pr-number. Based on the positive coefficient of the Re-number, an increasing Nu-number with increasing Re-number is predicted which corresponds to the experimental data dependent of the solution mass flow per unit length tube shown in figure 2.

The correlation of Sernas [1] is developed from experimental data determined on a single electrical heated horizontal tube and is actually only valid for tubes with an outer diameter of 25,4 mm. Further correlations for larger diameters are presented by Sernas but not for smaller ones. So this correlation is used for the comparison because it fits best to the tube diameter used in this work.

Hu and Jacobi [2] present a separate correlation for the single flow pattern of the falling film. Furthermore, the hydrodynamics of the droplets are considered by the Ar-number as well as the influence of the tube bundle geometry represented by the fraction of the inter-tube distance  $s$  and the outer tube diameter  $d$ .

The correlation presented by Jani [3] is developed from a numerical simulation of heat and mass transfer in a laminar falling over a single horizontal tube. LiBr solution with varying concentrations is used as working fluid in the simulation. The geometry of the tube is considered by a dimensionless diameter which is expressed by the relation between tube diameter and length. Jani directly couples heat transfer with diffusive mass transfer by the consideration of Sc-number in the Nu-correlation.

All correlations are used to calculate the heat transfer coefficient under the same boundary conditions as shown in figure 2 with exactly the same material properties for a comparison with the experimental data. The results are shown exemplarily in figure 4 for a heating water temperature of 75°C. The significant deviation between the experimental data and the results calculated with the correlation of Jani is relevant. This might be explained by the simplified boundary conditions under which the correlation of is developed. The heat transfer coefficients calculated by the correlation of Sernas are approximately in the same range as the experimental data but the influence of the mass flow rate is less strong compared to the experimental data. This difference may be a result of the tube diameter of the experimental investigated tube bundle which is smaller than the one for which the correlation is developed. The results calculated with the correlation of Hu and Jacobi for droplet flow are in good agreement with the experimental data. Even for a high solution mass flow the heat transfer characteristics are predicted quite well although the flow pattern changed during the experimental investigations from droplet mode to droplet-jet mode. The correlation for jet flow presented by Hu and Jacobi is applicable at the point on that jets appear, too. The results of both correlations are very close at a solution mass flow per unit length tube of 0,025 kg/ms. The transition area from droplet to jet flow can be described with an acceptable accuracy by both correlations.

All experimental data in comparison with the corresponding data predicted by the correlation of Hu and Jacobi for droplet mode are shown in figure 5 (left) in a dimensionless way. A good agreement between calculated and measured Nu-numbers is observed for every state although the predicted ones seems to be systematically lower than the measured ones. Furthermore, the increase of the Nu-number with increasing Re-number is more digressive in reality than calculated. This is valid especially for

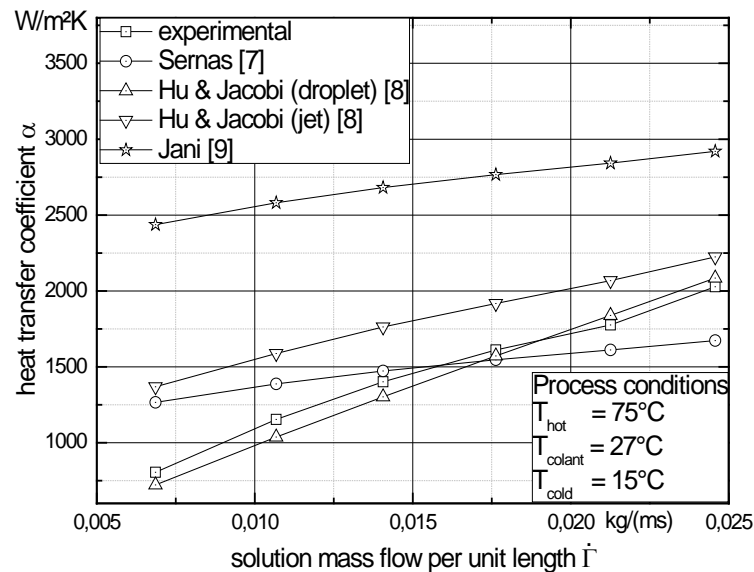


**Figure 4.** comparison of predicted and experimental heat transfer coefficients

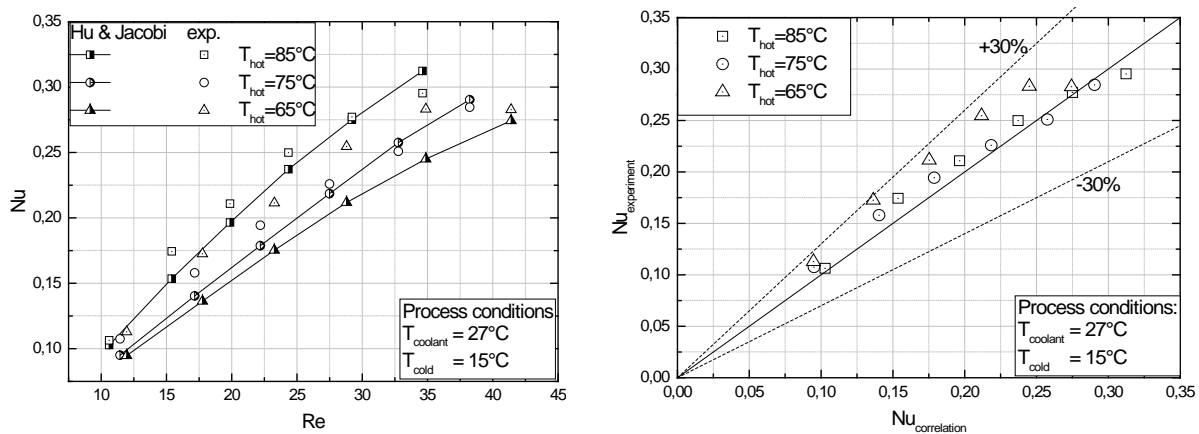


**Figure 5.** comparison of experimental and predicted Nu numbers(left); deviation between experimental and predicted Nu numbers(right)

higher Re-numbers. The deviation between the experimental and the calculated data is shown in figure 5 (right) where the experimentally determined Nu-number is plotted as a function of the calculated Nu-number. All experimental data are in good agreement with the predicted ones within a tolerance of 30%. Even in the transition area between droplet and jet flow the percental deviation falls in an acceptable range, although the correlation is not recommended for this flow pattern.

It may be concluded that the correlation of Hu and Jacobi for droplet mode in eq. (13) describes the heat transfer in a falling film evaporator with aqueous LiBr-solution at low pressure best compared to the other considered correlations. The correlation seems to be applicable for both a falling film in droplet mode and in the beginning transition mode between droplet and jet mode.

## 5. Conclusion

The heat and mass transfer characteristics of a horizontal tube bundle falling film evaporator working with aqueous LiBr-solution are analysed. An increase of the Nu-number with increasing Re-number is observed. An impact of the flow pattern in the falling film on the heat transfer is shown. It is shown that the Nu-number is stronger dependent on the Re-number for droplet mode than for jet mode.

A good agreement of the experimental data with the heat transfer coefficient predicted with the correlation of Hu and Jacobi for droplet mode is shown when comparing several correlations from the

literature. The heat transfer coefficient can be calculated by the correlation within a deviation of 30% from those of the experimental examination. The results indicate an applicability of the correlation for falling film evaporation in droplet mode as well as in beginning transition mode from droplet to jet mode.

## Nomenclature

### Latin

A	Area (m <sup>2</sup> )	l	Length (m)
c <sub>p</sub>	isobaric specific heat capacity (kJ/kgK)	m	mass flux (kg/s)
d	diameter (m)	p	Pressure (mbar)
D*	dimensionless diameter (-)	Q	heat flux (W)
g	acc. of gravity (m/s <sup>2</sup> )	s	inter-tube spacing (m)
j	number (-)	T	temperature (K)
k	overall heat transfer coefficient (W/m <sup>2</sup> K)	x	Concentration (kg <sub>LiBr</sub> /kg <sub>solution</sub> )

### Dimensionless parameters

Ar	Archimedes number	Re	Reynolds number
Nu	Nusselt number	Sc	Schmidt number
Pr	Prandtl number		

### Greek

α	heat transfer coefficient (W/m <sup>2</sup> K)	λ	heat conductivity (W/mK)
Γ	mass flow per unit length (kg/ms)	ξ	friction factor (-)
η	dynamic viscosity (Pas)	ρ	density (kg/m <sup>3</sup> )

### Subscripts

cu	copper	h	hot water	lm	log. mean	s	solution
f	film	i	inlet / internal	o	outer/outlet		

## References

- [1] Sernas, V.: Heat Transfer Correlation for Subcooled Water Films on Horizontal Tubes. Journal of Heat Transfer Vol. 101, Feb. 1979
- [2] Hu, X.; Jacobi, A.M.: The Intertube Falling Film: Part 2 – Mode Effects on Sensible Heat Transfer to a Falling Liquid Film. Journal of heat Transfer Transactions of the ASME, Vol. 118, Aug 1996. S. 626-633
- [3] Jani, S.: Simulation of Heat and Mass Transfer Process in Falling Film Single Tube Absorption Gernerator. International Journal of Science and Engineering Investigations Vol. 1, Issue 3, Apr 2012, S. 79-84
- [4] Olbricht M., Luke A.: Investigation of the Operation Conditions of an Absorption Cycle with compact Heat Exchangers, International Sorption Heat Pump Conference March 31- April 3 2014 Washington
- [5] Olbricht, M.; Luke, A.: Prediction an experimental investigation of heat and mass transfer charactersitics of a horizontal tube bundle absorber, International Congress of Refrigeration, 2015, Yokohama
- [6] Patek J., Klomfar, J. 2006, A computationally effective formulation of the thermodynamic properties of LiBr-H<sub>2</sub>O from 273 to 500 K over full composition range International Journal of Refrigeration 29: 566-578
- [7] Gnielinski V.: New Equations for Heat and Mass Transfer in Turbulent Pipe and Channel Flow, Int. Chem. Eng., Vol. 16, pp. 359-368, 1976
- [8] Serth. W. R.: Process Heat Transfer – Principles and Applications; Elsevier, 2007 Apr 2012, pp. 79-84